Inorganic Materials, Vol. 40, No. 4, 2004, pp. 415–419. Translated from Neorganicheskie Materialy, Vol. 40, No. 4, 2004, pp. 486–490.

# Synthesis and Properties of Phases in the System $BaCO_3$–PbO–$Nb_2O_5$

**S. A. Shtin, A. L. Podkorytov, V. M. Zhukovskii,**
**E. V. Sokolova, and S. R. Kudakaeva**
*Ural State University, pr. Lenina 51, Yekaterinburg, 620083 Russia*
*e-mail: anatoliy.podkorytov@usu.ru*
Received April 15, 2003

**Abstract**—The phase formation kinetics and phase relations in the $BaCO_3$–PbO–$Nb_2O_5$ system are studied. Barium lead niobates are prepared by solid-state reactions, and the composition ranges of solid solutions with different structures are determined. All of the materials are examined by x-ray diffraction, and their stability in acid media is assessed. The electrical conductivity of the Pb-containing niobates is measured. The results are used to analyze property–structure–composition relations. Based on the phase-equilibrium data and the chemical stability and electrical properties of the niobates, the structure types and compositions of niobates are identified which are the most attractive for producing ion-selective materials.

## INTRODUCTION

Our previous studies [1–3] showed that niobates are potential materials for ion-selective electrodes. Clearly, precise knowledge of their chemical, structural, and electrochemical properties is critical for this application. Detailed investigation of Ni- and Pb-containing strontium niobates [4] culminated in the fabrication of ion-selective electrodes with good performance parameters [2, 3]. The objective of this work was to prepare new electrode materials based on Pb-containing alkaline-earth niobates for ion-selective meters.

## EXPERIMENTAL

The starting reagents used in solid-state synthesis are listed in Table 1. The reagents were precalcined in order to remove residual moisture and obtain stable modifications.

The starting mixtures were placed in alundum crucibles and reacted in air in Silit furnaces with multiple intermediate grindings in 2-propanol. During synthesis, the temperature was raised stepwise. The temperature was maintained with an accuracy of ±5°C and was measured by Pt/Pt–Rh thermocouples connected to an F-295-4 voltmeter.

The phase composition of the samples and the stoichiometry ranges of solid solutions were determined by x-ray diffraction (XRD) on a DRON-2.0 powder diffractometer (Cu$K_\alpha$ radiation). The final synthesis temperatures ($t_s$) and solid-solution ranges are listed in Table 2.

The reaction onset temperature ($t_0$) and the temperature range of active reaction ($\Delta t$) were determined by thermal analysis (TG + DTA) of $BaCO_3 + PbO + Nb_2O_5$ mixtures during heating to 1050°C, using a Q-1500D thermoanalytical system (Table 3) interfaced with an AMD K6-2-333 PC for measurement automation and data processing. The reaction kinetics were followed using isothermal gravimetry. The experimental setup included a VLA-200M analytical balance, heater, power supply, temperature controller, and temperature-measuring system. Conversion was inferred from weight loss data; the rate-limiting step was identified by the reduced coordinate method [5].

Samples for conductivity measurements were prepared by pressing powdered materials into pellets 10 mm in diameter, which were sintered first at 800°C and then at the highest synthesis temperature for 4 h.

After grinding the faces of the pellets, electrical contacts were formed by depositing ammonium hexachloroplatinate, which was then decomposed above 300°C to give fine-particle platinum:

$$(NH_4)_2PtCl_6 \longrightarrow 2NH_3\uparrow + 2HCl\uparrow + 2Cl_2\uparrow + Pt.$$

Electrical conductivity was measured by a two-probe technique at 1 kHz during cooling in air, using an

**Table 1.** Starting reagents and calcination temperatures (calcination time, 3 h)

| Reagent | Grade | Calcination temperature, °C |
|---|---|---|
| $Nb_2O_5$ | OSCh 7-3 | 1200 |
| $BaCO_3$ | OSCh 7-2 | 600 |
| PbO | Analytical grade | 500 |

**Table 2.** Structure, composition, and stoichiometry ranges of solid solutions in the $BaCO_3$–PbO–$Nb_2O_5$ system

| Structure type, symmetry | Chemical composition | Stoichiometry range | $t_s$, °C |
|---|---|---|---|
| Cryolite, cubic | $Ba_{6-x}Pb_xNb_2O_{11}$ | $0 < x \leq 0.5$ | 1450 |
| Perovskite, cubic | $Ba_{3-x}Pb_xNb_2O_8$ | $0 < x < 0.1$ | 1200 |
|  | $Ba_{4-x}Pb_xNb_2O_9$ | $0 < x \leq 0.5$ | 1400 |
| Hexagonal | $Ba_{5-x}Pb_xNb_4O_{15}$ | $0 < x \leq 0.4$ | 1400 |
| Calcium tantalate, orthorhombic | $Ba_{1-x}Pb_xNb_2O_6$ | $0 < x \leq 0.1$ | 1250 |
| Tetragonal tungsten bronze (TTB), tetragonal | $Ba_{2-x}Pb_xNb_{10}O_{27}$ | $0 < x \leq 0.2$ | 1150 |
| Pyrochlore, tetragonal | $Pb_{3-x}Ba_xNb_2O_8$ | $0 < x \leq 0.5$ | 1200 |

RLC meter and a standard cell with platinum current leads, which were pressed against the contacted faces. The temperature was monitored with a Pt/Pt–10% Rh thermocouple connected to an F-295-4 voltmeter. Readings were taken every 10°C. Repeated measurements showed good reproducibility of results. The accuracy in our conductivity measurements was 1%. The total ionic transference numbers $\Sigma t_i$ in the constituent niobates were evaluated earlier from emf measurements [6].

## RESULTS AND DISCUSSION

According to our results, $BaCO_3$ does not decompose below 1050°C (Table 3). Therefore, any weight losses in $BaCO_3$-containing reaction mixtures below this temperature are due to $CO_2$ release by virtue of chemical interaction with other components.

The introduction of PbO into reaction mixtures containing $Nb_2O_5$ and $BaCO_3$ typically reduces $t_0$. Moreover, increasing the PbO content reduces $\Delta t$ (Table 3).

The introduction of PbO notably accelerates solid-state reactions. The reduced coordinate method (Fig. 1) was used to identify the rate-limiting process at different reaction stages. In all of the reaction mixtures, we revealed a transition, at different conversions, from direct chemical reaction to diffusion control (Table 4), which is well described by the Ginstling–Brownshtein equation under the assumption that the reactants consist of spherical particles [5],

$$D(\alpha) = \left[1 - \frac{2}{3}\alpha - (1-\alpha)^{2/3}\right] = \frac{2K\tau}{R^2} = K\tau,$$

where $\alpha$ is conversion, $K$ is the reaction rate constant, $R$ is the particle radius of the component being covered, and $\tau$ is the reaction time.

Some of the Pb-containing barium niobates have a broader homogeneity range (Table 2) than their strontium analogs [4]. Moreover, Pb-doped barium niobates are more stable in acid media than Pb-substituted strontium niobates, which is of importance in pH measurements. The highest stability in acidic aqueous solutions is offered by niobates with the TTB structure.

Figure 2 shows the Arrhenius plots of conductivity for $Ba_{n-x}Pb_xNb_{2y}O_{5y+n}$. For comparison, Fig. 3 shows the composition dependences of conductivity for the parent barium niobates. Table 5 compares the conductivities of niobates and the activation energies for conduction above and below the break point.

The conductivity of Pb-containing barium niobates decreases with increasing Pb content (Fig. 3). The highest conductivity is offered by the $Ba_{6-x}Pb_xNb_2O_{11}$ (cryolite structure) and $Ba_{2-x}Pb_xNb_{10}O_{27}$ (TTB structure) solid solutions. The conductivity of $Ba_{4-x}Pb_xNb_2O_9$, $Ba_{5-x}Pb_xNb_4O_{15}$, and $Ba_{1-x}Pb_xNb_2O_6$ is somewhat lower. A similar relationship holds for the undoped barium niobates. For all of the solid solutions studied, we determined the activation energy for conduction (Table 5).

**Table 3.** Thermal analysis data for reaction mixtures

| Composition | $t_0$, °C | $\Delta t$, °C |
|---|---|---|
| $BaCO_3$ | >1050* | – |
| $4BaCO_3 + 2PbO + Nb_2O_5$ | 745 | 820–1050 |
| $5BaCO_3 + PbO + Nb_2O_5$ | 810 | 970–1050 |
| $4.8BaCO_3 + 0.2PbO + 2Nb_2O_5$ | 845 | 950–1050 |
| $0.8BaCO_3 + 0.2PbO + Nb_2O_5$ | 890 | 945–1050 |
| $2BaCO_3 + 5Nb_2O_5$ | 900 | 990–1050 |
| $1.8BaCO_3 + 0.2PbO + 5Nb_2O_5$ | 760 | 880–1050 |

* Thermolysis onset.

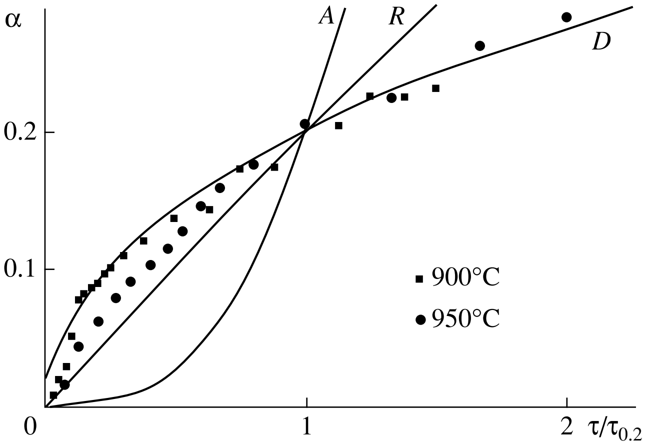

**Fig. 1.** Reaction kinetics in a $3.5BaCO_3 + 0.5PbO + Nb_2O_5$ mixture. The solid lines represent theoretical fits for different rate-limiting processes: (*A*) nucleation, (*R*) chemical reaction, (*D*) diffusion through the layer of the reaction product.

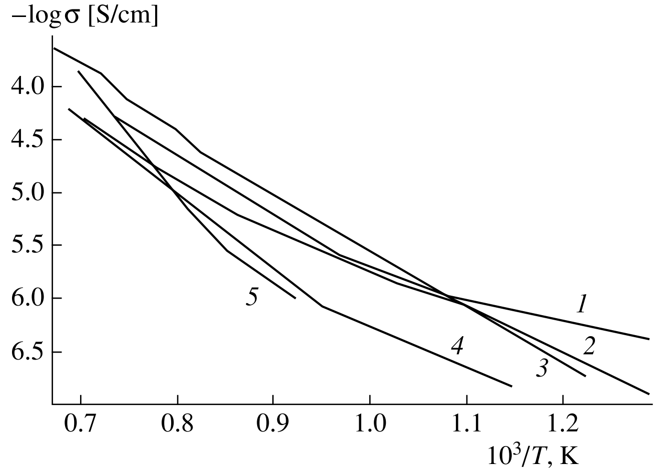

**Fig. 2.** Arrhenius plots of conductivity for (*1*) $Ba_4Pb_2Nb_2O_{11}$, (*2*) $Ba_{3.5}Pb_{0.5}Nb_2O_9$, (*3*) $Ba_{0.9}Pb_{0.1}Nb_2O_6$, (*4*) $Ba_{4.6}Pb_{0.4}Nb_4O_{15}$, and (*5*) $Ba_{1.8}Pb_{0.2}Nb_{10}O_{27}$.

Some of the Pb-containing barium niobates have a higher conductivity than their strontium analogs [4] and are, therefore, of practical interest. In particular, there is considerable interest in new materials for ion-selective electrodes. Some of the niobates studied here meet the main requirements for such materials [7–9]. The attractive properties of niobates ceramics, such as high phase purity, stability in acid media in a broad pH range,

**Table 4.** Isothermal gravimetry data for $BaCO_3$–PbO–$Nb_2O_5$ samples

| Composition | *t*, °C | $\alpha_{max}$, % | Type of control |
|---|---|---|---|
| $0.8BaCO_3 + 0.2PbO + Nb_2O_5$ | 850 | 19 | *D* |
| | 900 | 41 | *D* |
| | 950 | 65 | *R* (α < 25), *D* (α > 30) |
| $3BaCO_3 + PbO + Nb_2O_5$ | 800 | 10 | *D* |
| | 900 | 32 | *D* |
| | 950 | 62 | *D* |
| $3.5BaCO_3 + 0.5PbO + Nb_2O_5$ | 800 | 8 | *D* |
| | 900 | 23 | *D* |
| | 950 | 42 | *RD* (α < 15), *D* (α > 15) |
| $4.8BaCO_3 + 0.2PbO + Nb_2O_5$ | 850 | 9 | *D* |
| | 900 | 27 | *D* |
| | 950 | 73 | *R* (α < 20), *D* (α > 20) |
| $4BaCO_3 + 2PbO + Nb_2O_5$ | 800 | 13 | *D* |
| | 850 | 71 | *R* (α < 35), *D* (α > 35) |
| | 900 | 76 | *R* (α < 40), *D* (α > 40) |

Note: *D* denotes diffusion control, described by the Ginstling–Brownshtein equation, and *R* denotes kinetic control, described by the contracting-sphere equation [5].

**Table 5.** Electrical properties of niobates

| Composition | $-\log\sigma$ [S/cm] |  | $\varepsilon$, eV |  | $t_{break}$, °C (±5°C) |
|---|---|---|---|---|---|
|  | 1150°C | 650°C | $t > t_{break}$ | $t < t_{break}$ |  |
| $Ba_6Nb_2O_{11}$ | 2.70 | 4.32 | 0.80 | 1.00 | 640 |
| $Ba_4Pb_2Nb_2O_{11}$ | 3.75 | 6.05 | 1.26 | 1.00 | 640 |
| $Pb_3NiNb_2O_9$ | 1.78 | 3.08 | 1.38 | 1.16 | 700 |
| $Ba_4Nb_2O_9$ | 3.45 | 4.90 | 0.90 | 0.90 | – |
| $Ba_{3.5}Pb_{0.5}Nb_2O_9$ | 4.45 | 5.86 | 1.85 | 0.34 | 880 |
| $Ba_5Nb_4O_{15}$ | 3.90 | 6.30 | 1.92 | 1.19 | 1020 |
| $Ba_{4.6}Pb_{0.4}Nb_4O_{15}$ | 4.37 | 6.68 | 1.33 | 0.49 | 650 |
| $BaNb_2O_6$ | 2.60 | 5.60 | 2.78 | 0.72 | 960 |
| $Ba_{0.9}Pb_{0.1}Nb_2O_6$ | 3.82 | – | 2.37 | 1.45 | 930 |
| $Ba_2Nb_{10}O_{27}$ | 3.91 | 6.86 | 1.90 | 0.74 | 750 |
| $Ba_{1.8}Pb_{0.2}Nb_{10}O_{27}$ | 3.99 | 6.08 | 2.87 | 0.80 | 750 |
| $PbNb_2O_6$ | 4.02 | 5.75 | 1.73 | 1.18 | 760 |
| $Pb_{2.5}Ba_{0.5}Nb_2O_8$ | 2.77 | 4.26 | 1.20 | 0.70 | 1110 |

mixed conductivity, framework–channel structure favorable for reversible exchange processes, and good mechanical strength, make them potential materials for membranes of ion-selective electrodes.

According to preliminary tests, the potential of thin-film ion-selective electrodes based on Pb-containing niobates (with polystyrene as an inert matrix) is sensitive to the concentration of Pb ions in solution [10].

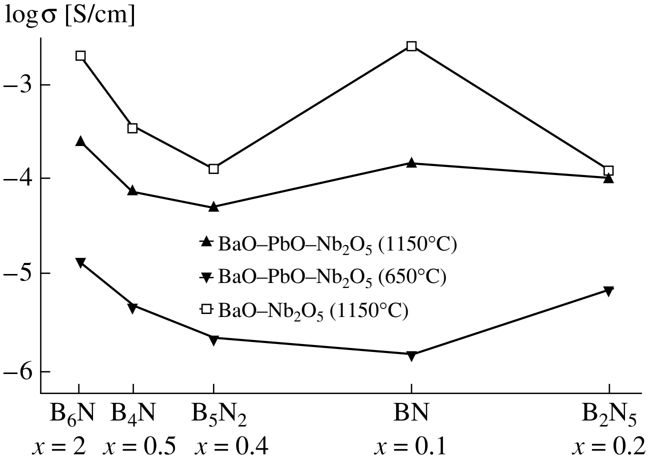

**Fig. 3.** Composition dependences of conductivity for barium niobates and Pb-containing niobate solid solutions: B = $Ba_{n-x}Pb_xO_n$, N = $Nb_2O_5$.

## ACKNOWLEDGMENTS

This work was supported by the Russian Foundation for Basic Research (grant R2002 URAL, no. 02-03-96457) and the US Civilian Research and Development Foundation (grant EK-005-XI).

## REFERENCES

1. Podkorytov, A.L., Pantyukhina, M.I., Shtin, S.A., and Zhukovskii, V.M., Synthesis and Properties of Nickel-Containing Niobates, *Zh. Neorg. Khim.*, 1999, vol. 44, no. 5, pp. 855–858.
2. Zhukovskii, V.M., Podkorytov, A.L., Sokolova, E.V., and Shtin, S.A., New Nickel and Lead Selective Electrodes, *Vserossiiskaya konferentsiya po aktual'nym problemam analiticheskoi khimii* (All-Russia Conf. on Critical Issues in Analytical Chemistry), Moscow, 2002, vol. 2, pp. 158–159.
3. Podkorytov, A.L., Shtin, S.A., Zhukovskii, V.M., *et al.*, Electrical Transport and Electrode Processes in Binary and Ternary Niobates, *V Mezhdunarodnoe soveshchanie po fundamental'nym problemam ioniki tverdogo tela* (V Int. Conf. on Basic Problems in Solid-State Ionics), Chernogolovka, 2000, pp. 150–154.

4. Podkorytov, A.L., Shtin, S.A., Zhukovskii, V.M., *et al.*, Electrical Transport in Nickel- and Lead-Containing Strontium Niobates, *Zh. Neorg. Khim.*, 2002, vol. 47, no. 11, pp. 1782–1786.
5. Delmon, B., *Introduction à la cinétique hétérogène*, Paris: Technip, 1969. Translated under the title *Kinetika geterogennykh reaktsii*, Moscow: Mir, 1972.
6. Neiman, A.Ya., Podkorytov, A.L., Animitsa, I.E., *et al.*, Cation Self-diffusion and Synthesis of Strontium and Barium Niobates, *Zh. Neorg. Khim.*, 1987, vol. 32, no. 2, pp. 359–365.
7. Volkov, V.L. and Gyrdasova, O.I., Nickel-Selective Electrode, *Zh. Anal. Khim.*, 1997, vol. 52, no. 8, pp. 844–847.
8. Nikol'skii, B.P. and Materova, E.L., *Ionoselektivnye elektrody* (Ion-Selective Electrodes), Moscow: Mir, 1980.
9. Camman, K., *Das Arbeiten mit ioneselektiven Elektroden*, Berlin: Springer, 1977. Translated under the title *Rabota s ionoselektivnymi elektrodami,* Moscow: Mir, 1980.
10. Sokolova, E.V., Shtin, S.A., Zhukovskii, V.M., *et al.*, Preparation and Properties of Lead-Containing Mixed Oxides, *VIII Vserossiiskoe soveshchanie po vysokotemperaturnoi khimii silikatov i oksidov* (VIII All-Russia Conf. on the High-Temperature Chemistry of Silicates and Oxides), St. Petersburg, 2002, p. 170.